

Robust Localization of an Arbitrary Distribution of Radioactive Sources for Aerial Inspection

Dhruv Shah

Department of Electrical Engineering
Indian Institute of Technology, Bombay
Mumbai, India – 400076
dhruv.shah@iitb.ac.in

Sebastian Scherer

Robotics Institute
Carnegie Mellon University
Pittsburgh, PA – 15217
basti@andrew.cmu.edu

ABSTRACT

Radiation source detection has seen various applications in the past decade, ranging from the detection of dirty bombs in public places to scanning critical nuclear facilities for leakage or flaws, and in the autonomous inspection of nuclear sites.

Despite the success in detecting single point sources, or a small number of spatially separated point sources, most of the existing algorithms fail to deliver in complex scenarios involving a large number of point sources or non-trivial distributions & bulk sources. Even in simpler environments, most existing algorithms are not scalable to larger regions and/or higher dimensional spaces. In a setup for autonomous inspection, we would be required to estimate not only the positions of the sources, but also the number, distribution and intensities of each of them.

In this report, we present a novel algorithm for the robust localization of an arbitrary distribution of radiation sources using multi-layer sequential Monte Carlo methods coupled with suitable clustering algorithms. We aim to achieve near-perfect accuracy, in terms of F1-scores, while allowing the algorithm to scale, both to larger regions in space, and to higher dimensional spaces.

I. INTRODUCTION

With the growing advent of nuclear sites and the need for the proper management and disposal of radioactive waste, there is an increasing demand for robust mechanisms to perform autonomous inspection of the disposal sites for the analysis of the waste, from time to time. Such a mechanism would require the *multi-modal mapping* of the environment, including an accurate estimate of the

distribution and intensities of the radioactive materials, using either ground or aerial robots. For the autonomous inspection purposes, we would like the robot to identify regions of interest, based on visual imagery, thermal imagery, radioactive heatmap, waste estimates etc., and map such regions with greater precision.

For the purpose of generating radiation map, the robot would have to identify the position and estimates of the sources of radioactivity, which tend to be very high in nuclear waste dump-yards. Most of the existing algorithms stop at the localization of multiple point sources, and cannot extend to a large number of such sources. The problem of localizing bulk sources and complex distributions lies unaddressed in literature.

The availability of very sophisticated gamma imaging cameras makes the task of localization pretty simple, by generating a likelihood map of the source estimates. These sensors, however, (i) require very large exposure time, during which the robot must remain absolutely stationary, and (ii) weigh too much, of the order of kilograms. These two factors eliminate the possibility of mounting such a sensor on light-weight drones or quad-copters, and hence we are required to move to much simpler sensors, which are fast, light-weight and yet, accurate.

Our work focuses on developing a scalable algorithm for the robust localization of multiple radiation sources, irrespective of the distribution, using cheap light-weight *particle flux* detectors. We also look at various extensions to the simple source localization problem, by attempting to solve more complex scenarios, without changing the heart of the algorithm. We propose an improved version of

a hybrid formulation of a particle filter (sequential Monte Carlo method) and clustering techniques to address and tackle the aforementioned challenges. In our method, we begin by generating hypotheses about source positions (*particles*); when a new measurement is received, the likelihoods of the hypothesis to be a real source is evaluated. Unlike a traditional particle filter, we *selectively* evaluate the particles based on their influence at the sensor that generated the reading. We also allow for multiple source localization by updating the *prediction* stage of the particle filter, and by reinforcing the algorithm using partially resolved sources in the environment. This notion of partially resolving the sources is key to the performance of the algorithm in complex scenarios.

Our main contributions are as follows:

- We propose an improved localization approach for multiple sources in complex environments and distributions that (i) can resolve large number of sources efficiently, (ii) is scalable to large regions in space and to higher dimensions, and (iii) can be used to identify and localize bulk radiation sources.
- We introduce the notion of *candidate sources*, which are source parameter estimates obtained after clustering. These are then evaluated based on a confidence metric, before labeling. This allows the algorithm to have a very high accuracy.
- The algorithm allows for partial localization of the sources in the environment, which can be used to reinforce the further iterations, simplifying it in the process. In this way, the problem of localization of large, complex environments is sequentially broken down to smaller simpler scenes, allowing improvement in performance over time.

The balance of the report is organized as follows. The related work in the field of radioactive source localization and the state-of-the-art are described in section II. In section III, we formulate the problem mathematically and introduce the concept of Bayesian filtering and recursive Bayesian methods, before presenting the proposed algorithm in detail. Section IV details some of the sample runs on the algorithm, by extending it to higher dimensional spaces and more complex environments. This is followed by the quantitative analysis of the algorithm and a comparative study against the state-of-the-art. We then conclude with future prospects, in section V.

II. RELATED WORK

The problem of $1/R^2$ -type source localization has been followed quite extensively in literature, in the contexts of acoustics, radio transceivers, electromagnetic fields, chemical plumes and also for radiation sources.

The classical problem of single source localization with known source intensity has been approached well by least squares fitting [14], maximum likelihood estimation (MLE) methods, which search the parameter space for the most likely source parameters [12]. Authors in [22] adapt a TDoA-based algorithm in log-space to exploit the logarithmic differences in source strength measurements to infer the source position. These algorithms assume a strong prior on the source intensity, and hence, are impractical in an inspection setup. [2] uses a ML-localization framework for the localization of a source with unknown intensity, guaranteeing no false stationary points as long as the source lies in the open convex hull formed by the sensors. These algorithms are not applicable in scenarios involving multiple point sources.

For localizing multiple sources, most existing algorithms must estimate the number of sources N_s , in addition to the existing source parameters. In [18], [17], the authors begin by estimating the number N_s using Gaussian mixture model based selection, and then compute the source parameters using the MLE method. As quoted in [17], the accuracy of the model selection degrades with increasing N_s ; also, the runtime blows up with the number of sources. A similar approach is used in [10], where targets are modeled with Gaussian mixture models, followed by Akaike's/Bayesian Information Criteria to estimate N_s . This is followed by a simple expectation maximization routine and clustering, to estimate the parameters. As quoted in [17], these EM or MLE based algorithms do not scale beyond four sources.

In [3], authors propose the multiple source localization by performing the gradient descent optimization of non-convex cost functions, assuming that the sources lie in the convex hull formed by the sensor positions. In [5], the authors propose to solve the localization problem using convex optimization, assuming that the sources are located in a grid over the region of interest. As reported in [5], the proposed algorithm proceeds by discretizing the search space and localizing in the discretized locations. In a reported case with one source and 196 sensors, the algorithm takes 209s to converge, which blows up to 3205s with 4 sources. Clearly, the algorithm fails in scaling to more complex distributions.

Another interesting approach was proposed in [19], using partial Bayes factors to evaluate the models. The use of Monte Carlo methods allows for more interesting implementations using traditional particle filters [4], which are used to approximate the source distribution for complex environments. Although this implementation does not scale very well, it served as a good alternative for the source parameter estimation. With significant updates to the estimation stage, *Rao et al.* [6] proposes an improvised particle filter that can be used for localizing a small number of point sources efficiently, and can scale to moderately large regions.

III. METHODS

This section details our sequential Monte Carlo implementation for an improved particle filter. For the sake of illustration, we assume the environment to be a two-dimensional grid containing point sources, which shall later be extended to higher dimensional spaces. We start off by describing the problem formulation and the sensor model used, and then give a brief on recursive Bayesian estimation, before presenting the algorithm.

A. Problem Formulation

We consider the localization of N_s radiation point sources of unknown strengths using a mobile ground/aerial robot in a two-dimensional plane around the target area with obstacles. Continuing the notation scheme used by *Rao et al.* [6], let $\mathcal{A} = \{\mathbf{A}_1, \dots, \mathbf{A}_{N_s}\}$ denote the set of radiation sources. Each such source is parametrized by a three-value vector $\mathbf{A}_k = \langle A_k^x, A_k^y, A_k^{str} \rangle$, for $1 \leq k \leq N_s$. The parameters, thus, define the position (x, y) in cm and strength A^s in microCuries (μCi) of the radiation source in concern. For more complicated cases, the parameter vector \mathbf{A}_k can be extended to account for position in 3D (A_k^z) or for more complex source distributions by appending terms corresponding to dipole and quadrupole moments of the source (described later).

1) *Radiation Measurement:* Ionising radiation (ionizing radiation) is radiation that carries enough energy to free electrons from atoms or molecules, thereby ionizing them. Ionizing radiation is made up of energetic subatomic particles, ions or atoms moving at high speeds (usually greater than 1% of the speed of light), and electromagnetic waves on the high-energy end of the electromagnetic spectrum. [24]

The task of measurement of radiation intensity can be seen as the task of measuring either of the

following: particle flux, energy fluence, beam energy, Kerma or dose. Each of these present different approaches to representing the ionization strength of the emitter. For the purpose of this research, we suppose the simplest model for measurement - measuring the *particle flux* or *source influence* at different points in space.

In a surveillance area without obstacles, the contribution of \mathbf{A} in the intensity recorded at a location x is

$$\mathcal{I}(x, \mathbf{A}) = A^s \left(h^2 + |x - A^{pos}|^2 \right)^{-1} \quad (1)$$

where h is the height of the sensor from the ground, and $A^{pos} = (A^x, A^y)$. The values (h, A^x, A^y) are obtained from the odometry measurements in the reference frame of the robot. Eqn. (1) is a model widely used in existing work and has been verified experimentally.

2) *Sensor Modeling:* The most common type of sensor is the Gieger counter, which identifies alpha, beta and gamma rays using the ionization effect in produced in a Geiger-Muller tube. Scintillators, as the name suggests, are excited by ionizing radiation, absorb its energy and scintillate. The resulting energy can be observed as electric pulses and coupled with a counter. This class of devices measures the *particle flux*, which is basically a measure of the strength of the radiation source at the point of measurement. Another such sensor is the semiconductor detector, which involves the excitation of a Silicon-based device by the ionizing radiation.

On the other side of the spectrum, there exist sophisticated portable gamma imaging cameras, much like the ones used for medical imaging for internal organs. One such instrument is the *Polaris-H*, which uses layers of CdZnTe crystals to give a cone of likelihood of the source [7], instead of simply giving the flux measurement. Such sensors tend to be very bulky and require exposure times of the order of 10 minutes to form accurate imagery. Due to these limitations, we restrict ourselves to using point radiation sensors, measuring particle flux, for the rest of this report. In particular, Silicon detectors and scintillators can be modeled simple manner shown below.

Instead of a sensor network, as used in standard distributed approaches [6], [25], [20], a sensor/sensor-array is mounted on the mobile robot, which can trace a trajectory of choice. The intensity is usually reported in counts per second (CPS) or counts per minute (CPM). Let p_i denote the position at which a sensor reading was taken, in the ground frame. If the robot has multiple sensors, it may record multiple readings from the

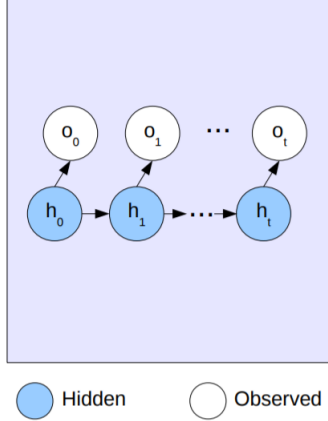


Fig. 1: A generic Bayesian filter graphical model, with observables o_i dependent on the hidden states h_i .

same position of the robot, but the sensors would be at distinct positions in the absolute frame. The sensor, at each position i , will record a background radiation B_i , that is naturally present due to cosmic rays and naturally occurring radio isotopes. This reading is usually very low (few CPM) and should not affect the model, but has been considered for the sake of completeness. The sensors have a different efficiency in counting the number of ionizations (hereby referred to as *interactions*) due to the difference in manufacturing technologies, processes, sizes etc. This can be incorporated using a calibration constant E_i . Given all of the above, the expected intensity (in CPS) at p_i can be given by

$$I_i = 3.7 \times 10^4 \times E_i \sum_{j=1}^{N_s} \mathcal{I}(p_i, \mathbf{A}_j) + B_i \quad (2)$$

The constant 3.7×10^4 is the conversion factor from microCurie to CPS (Becquerel). Given the expected intensity I_i , the measurements received by the sensor i , $m(S_i)$ are modeled as a Poisson process with average rate $\lambda = I_i$, which is known to be the distribution followed by photon intensities [13].

B. Bayesian Estimation

The problem of source localization can be viewed as that of the mapping problem in SLAM. Hence, we model the scenario in a similar fashion. Consider the general state space model with hidden variables $\mathbf{h}_t = \{h_0, h_1, \dots, h_t\}$ and observed variables $\mathbf{o}_t = \{o_1, o_2, \dots, o_t\}$; we would like to perform an inference on the hidden variables \mathbf{h}_t . Given the observed variables, Bayesian inference

on the hidden variables relies on the joint posterior distribution $p(\mathbf{h}_t | \mathbf{o}_t)$. The corresponding Bayesian belief network is shown in Figure 1. Assuming that the hidden variables have some initial distribution $p_0(h_0)$, a transition model $p(h_t | h_{t-1})$, and that the observations are *conditionally independent* given the hidden process (yielding the marginal distribution $p(o_t | h_t)$), a Bayesian filter can be used to derive a recursive expression for this posterior

$$p(\mathbf{h}_t | \mathbf{o}_t) = p(\mathbf{h}_{t-1} | \mathbf{o}_{t-1}) \frac{p(o_t | h_t) p(h_t | h_{t-1})}{p(o_t | \mathbf{o}_{t-1})} \quad (3)$$

which gives an expression for the update of the posterior, using the observables and the transition models. A formal proof to the above expression can be found in [11].

The above can be extended to a SLAM framework with the robot position and map as hidden variables $\mathbf{h}_t = \{\mathbf{x}_t, \Theta_t\}$, and the sensor measurements \mathbf{z}_t as a recursive update:

$$p(x_t, \Theta | \mathbf{z}_t) = \eta \, p(z_t | x_t, \Theta) \int p(x_t | x_{t-1}) p(x_{t-1}, \Theta | \mathbf{z}_{t-1}) dx_{t-1} \quad (4)$$

which indeed has the form of the recursive Bayesian filter, Eqn. 3.

Unfortunately, the computation of the integral over all robot positions x_{t-1} is intractable and hence, must be approximated. The most popular approximations involve the use of Kalman filters or particle filters. We shall look at the approach using particle filters in depth.

Traditional Particle Filter: Particle filters form a sequential Monte Carlo approximation to the recursive Bayesian filter described above. In addition, particle filters provide a usable implementation of Bayesian filtering for systems whose belief state and sensor, process noise can be modeled by non-parametric probability density functions [1].

In the traditional case, the particle filter can maintain a discrete approximation of the SLAM posterior using a large set of *particles*, or samples, in the state space. In this case, a weighted approximation of the recursive Bayesian filter can be given as:

$$p(s_t | \mathbf{z}_t, \mathbf{u}_t) \approx \sum_{i=1}^{N_s} w^{(i)} s_t^{(i)} \quad (5)$$

where we have a set of N_s particles $\{s^{(1)}, s^{(2)}, \dots, s^{(N_s)}\}$, with weights $w^{(i)}$. Assuming that we have such a set of weights and particles, we can update these particles by drawing samples from $q(\cdot)$:

$$s_t^{(i)} \sim q(s_t | s_{t-1}^{(i)}) \quad (6)$$

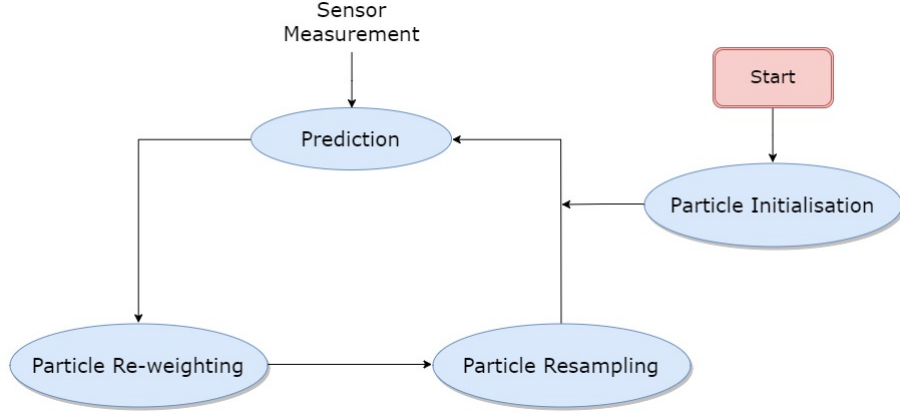


Fig. 2: Algorithmic flow for a traditional particle filter

where $q(x_t|x_{t-1}, z_t)$ is a distribution that is easy to sample, and approximates $p(x_t|x_{t-1}, z_t)$ with fatter tails, assuring the coverage of $p(\cdot)$. Thus, the weights are updated as:

$$w_t \propto w_{t-1} \frac{p(z_t|s_t)p(s_t|s_{t-1})}{q(s_t|s_{t-1}, z_t)} \quad (7)$$

In the optimal case, $q(\cdot) = p(\cdot)$, but since it may not be easy to sample from that distribution, we can instead use the motion model $p(x_t|x_{t-1})$, which allows us to simplify the weight update equation to

$$w_t \propto w_{t-1} p(z_t|s_t) \quad (8)$$

It is key to note that the core prediction step of the Bayesian filter (Eq. 5) poses a fundamental limitation in localizing multiple sources, which was modified by Rao *et al.* [6]. We will be building upon this improved model of the traditional particle filter (Figure 2) in the coming sections, but the underlying principle of importance sampling and Bayesian updates is critical and unchanged.

C. Proposed Algorithm

In this section, we describe our algorithm for the robust localization of an arbitrary distribution of radiation sources, given the particle flux measurements, using a mobile robot. The proposed algorithm recursively refines the source parameter estimates based on newly acquired measurements, and can localize fairly complex source distributions recursively. Figure 3 outlines the flow of the algorithm. The algorithm begins by spawning a collection of particles, randomly or based on a known prior, each of which hypothesizes the location and strength of a radiation source. At each new robot position, or alternatively, a new sensor reading, the algorithm identifies the particles in it's

area of influence and their weights are updated in a Bayesian manner, according to the newly received sensor measurement, and the prior weights. After weighting the particles, a resampling procedure normalizes the weights of the particles. The procedure then repeats as a new measurement arrives. At any point in this cycle, a list of candidate sources can be obtained by running a suitable clustering or labeling routine, which estimates the most likely source parameters.

The algorithm can reinforce its estimates after some of the sources have been resolved, enabling better accuracy for localizing a large number of sources. The outer loop, as seen in figure 3, illustrates how the algorithm improves with time, eventually localizing the whole scene. Some salient features of our formulation are as follows:

- We use the notion of a *time step*, which refers to the unit of time when the readings from all positions have been received and processed, i.e., the robot has successfully explored the environment.
- Instead of explicitly modeling different source distributions and interactions, we compute the parameter estimates for the particles independent of each other. This enables the algorithm to scale readily with the number of sources, unlike the exponential trends demonstrated by conventional methods.
- At any point in time, the source parameters can be computed by a suitable clustering algorithm. A candidate source with a good enough confidence score is declared as *resolved*, and the algorithm takes that into account in the subsequent steps. This allows more efficient localization of multiple sources, and at the same time, enables the algorithm to detect complex source distributions that could not be detected otherwise.

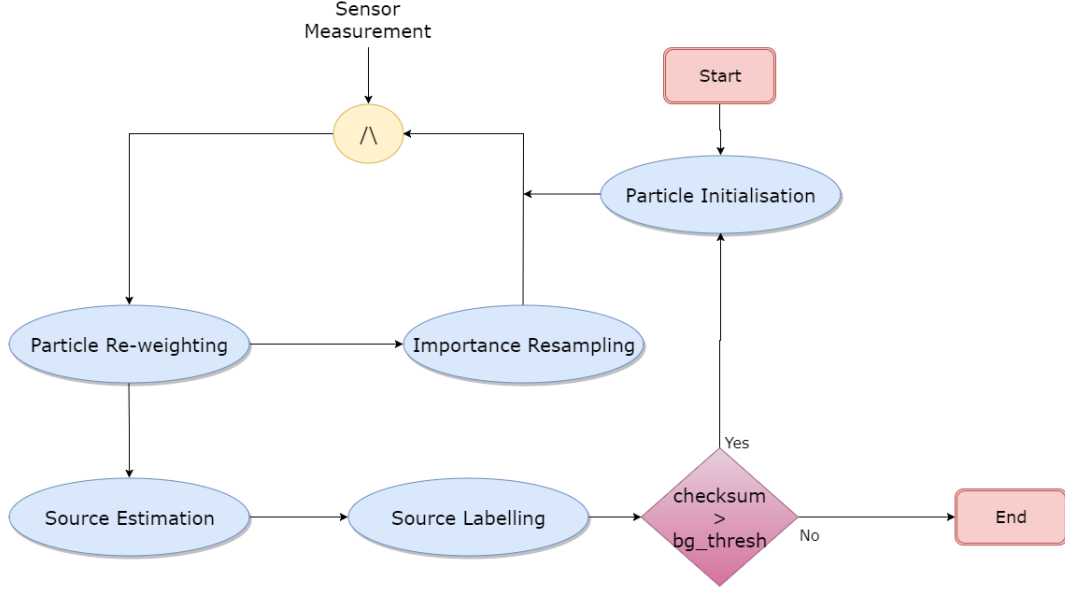


Fig. 3: Overview of the proposed algorithm

- At no point in time, does the algorithm require any a priori information than what has been stated. However, if such information is available for the source strengths, locations, or number, the convergence can be sped up by very large factors. The algorithm, despite being independent of any such assumptions, can be readily refined on provision of more information.
- Without loss of generality, the parameter vector of a particle can have any number of entries, like the z-coordinate, a dipole moment and dipole moment vector and so on. In principle, the algorithm would converge to the correct result in each case, but the number of time steps involved & particle population required would depend directly on the number of source parameters to be estimated.

The various stages of the algorithm are described in the sub-sections that follow.

1) *Particle Initialization:* At time step $t = 0$, the particle filter is initialized as follows. Let $\mathcal{P} = \{\mathbf{p}_i^{(t_i)} | i = 1, \dots, N_{\mathcal{P}}\}$ be a set of particles in the target area. Each particle $\mathbf{p}_i^{(t_i)}$ is a vector in the parameter space \mathbb{A} , denoting the position and source parameters of the hypothesized source. For the simplest case, it can be visualised as the three-value vector in \mathcal{A} . The superscript t_i is an integer denoting the time step at which the particle is being updated. In the general formulation, with no assumption on source strengths and positions, we initialize \mathcal{P} with uniformly random particles in the target area and a large window of source

strengths. If prior knowledge is available, the particles can be initialized according to the pre-existing distribution, greatly improving the performance of the algorithm. Some examples of such a guided initialization are shown in figure 4.

We denote the cardinality of \mathcal{P} , or the number of particles as $N_{\mathcal{P}} = |\mathcal{P}|$. This $N_{\mathcal{P}}$ directly governs the coverage of \mathcal{P} in \mathbb{A} , in a random initialization. A larger coverage will result in a more accurate estimate in a shorter time, because the Monte Carlo methods approximate the real distributions only when the number of particles being sampled is sufficiently large. In addition to the parameter vector, we associate each particle $p \in \mathcal{P}$ with a weight $w(\mathbf{p})$ such that $w(\mathbf{p}) \approx \sum_j P(\mathbf{A}_j = \mathbf{p})$ and $\sum_{\mathcal{P}} w(\mathbf{p}_i) = 1$. This weight measures the probability that an actual radiation source can have the same parameters as the concerned particle. Since the number $\sum_j P(\mathbf{A}_j = \mathbf{p})$ cannot be computed, it must be approximated. In the next subsection, we shall see how the weights are updated, so as to converge to the required number. For the initialization stage, each particle is assigned equal weight, given by $w(\mathbf{p}) = \frac{1}{N_{\mathcal{P}}} \forall \mathbf{p} \in \mathcal{P}$.

2) *Particle Reweighting:* This step forms the actual Bayesian estimation framework of the filter. Although we do not know the actual source parameters, we can estimate this probability using the sensor measurements. The particle filter under consideration is a sequential Monte Carlo approximation to the recursive Bayesian filter, as formulated in section III-B. Rephrasing eqn. 8 in this case, the weight of a particle \mathbf{p}_i can be updated

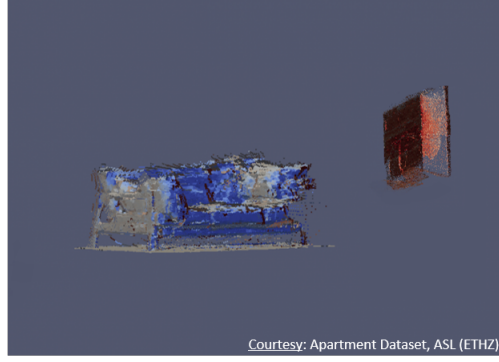
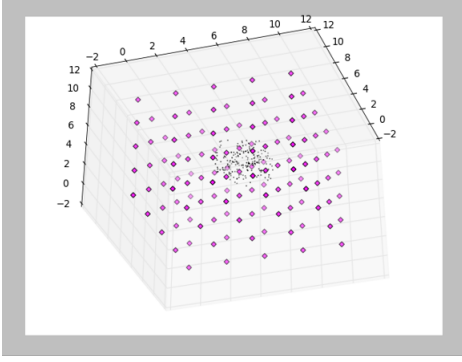


Fig. 4: Examples of guided particle initialization (a) in a simulated 3D environment, and (b) using point cloud data for a closed room.

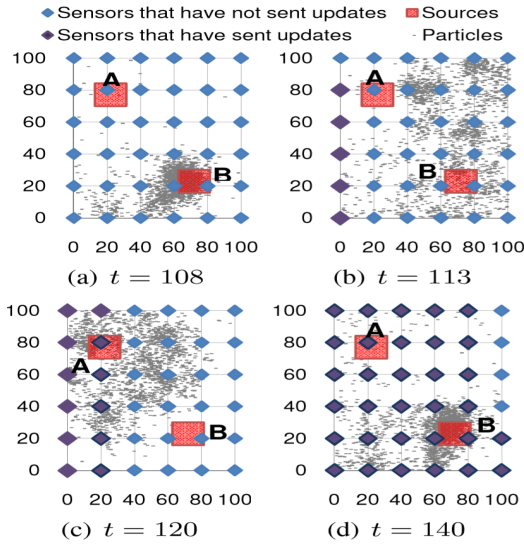


Fig. 5: Behaviour of the particles without fusion range.

as

$$w(\mathbf{p}_i^t) = p^*(m(S_i)|\mathbf{p}_i^t) \cdot w(\mathbf{p}_i^{t'}) \quad (9)$$

Here, the distribution $p^*(\cdot)$ represents a scaled-up version of $p(\cdot)$, the distribution obeyed by the radiation source. In particular, $p(x|y)$ stands for the probability of obtaining a value x , when sampling from a Poisson distribution with mean y . For this case, $p^*(x|y)$ can be given as

$$p^*(x|y) = \frac{p(\lfloor y \rfloor | y)}{f_y} \quad (10)$$

where $\lfloor \cdot \rfloor$ depicts the floor operator. f_y is the scaling factor which ensures that most accurate particles do not lose significant weight in the update step.

If we have prior information on any known

sources, or some sources (\mathbf{A}_k^*) have been resolved by the algorithm, Eqn. (9) can be modified to incorporate this information, and hence converge more efficiently, as follows.

$$w(\mathbf{p}_i^t) = p^*(m(S_i)|\mathbf{p}_i^t, (\mathbf{A}_k^*)) \cdot w(\mathbf{p}_i^{t'}) \quad (11)$$

Updating the weights of the particles, as above, for all particles in the target area, for each sensor, would be both computationally infeasible and impractical. For particles far away from a sensor, a small amount of uncertainty due to the sensor would cause a large reduction in weight, leading to the loss of a potential candidate. This is where the notion of *fusion range*, as proposed by Rao *et al.* comes handy. The notion of a fusion range is directly linked to the idea of *area of influence* of a source or sensor. The influence of a source at a given point falls off with the second order of the distance between them. This means that sensors sufficiently far enough do not exhibit a strong enough influence to have a say in the weight of a particle. Figure 5 provides a simple illustration of the phenomenon. Henceforth, we define the fusion range as a number d such that

$$\mathcal{P}' = \{\mathbf{p}_i | \|\mathbf{S}_i - \mathbf{p}_i^{pos}\|^2 \leq d^2\} \quad (12)$$

\mathcal{P}' is the set of particles lying within the fusion range of a sensor at location \mathbf{S}_i . Thus, Eqn. (9) is used to update the weights of every particle $\mathbf{p} \in \mathcal{P}'$. The sensor measurements close to the particles will provide a better view at those locations. By updating particles that are close to the sensor providing measurement only, we allow multiple sources to co-exist in a small neighborhood. Along with improving the accuracy of the estimation, this also enables us to increase the computational efficiency of the algorithm. The re-weighting step in Eqn. (9) only needs to be computed for particles in the fusion range, reducing the computational time by orders of magnitude.

In addition to the above, we maintain an entry called *checksum* for each time step. This is simply a number that stores the sum of readings registered by each sensor position, and can be seen as a simple method to identify the end point of source localization - if the checksum is negative (or *very small*), the algorithm has localized all sources. This is explained more clearly in section III-C5.

3) *Importance Resampling*: Importance resampling, or sampling importance resampling (SIS), are common practices used with Monte Carlo methods for the resampling stage of the filter [16]. In this step, we wish to replace particles of low weights with particles of higher weights, as a way to ensure a better convergence and prevent *particle degeneration*. In a particle filter without resampling, all the particles will have decreasing weights over time, except for the one closest to the source(s). Not only will this give an inaccurate estimate of the source parameters, it can also give spurious results.

Since the weight update was carried out only on particles within the fusion range \mathcal{P}' , the resampling shall also be done on the same set. The weights of the particles, defined and updated in sections III-C1 and III-C2, act as the importance distributions for the intended resampling procedure. This resampling is accomplished by sampling from \mathcal{P}' with probabilities $\frac{w(\mathbf{p}_i)}{\sum_{\mathbf{p}_j \in \mathcal{P}'} w(\mathbf{p}_j)}$ for all $\mathbf{p}_i \in \mathcal{P}'$. The resampled particles are then assigned uniform weights. This new set can be then merged with the original set of particles to give the updated set of particles, ready for the sensor reading from the upcoming iteration.

During the resampling process, irrespective of whether the particle is duplicated or not, we introduce some zero-mean Gaussian noise into each parameter of the generated particle. This noise serves a two-fold purpose: (i) it allows propagation of the particle in parameter space, allowing convergence to points that were not originally initialized in \mathbb{A} , and (ii) it ensures that particles are always slightly different, so that the filter does not always degenerate to a single point. The Gaussian nature of the noise can be exploited in the labeling stage, where a clustering technique like the mean-shift algorithm, which uses a multi-variate Gaussian kernel for grouping, can be fine-tuned to obtain near-optimal classification.

The above resampling procedure eliminates particles that do not correspond to any real sources, because their weights would degrade over time, and hence vanish. As time proceeds, areas with no radiation sources in the vicinity would have little or no particles around them. If the environment was

dynamic, and a new source was to move into that region, it could go undetected. To account for this scenario, we randomly replace a small percentage of particles, say 5-10%, with random particles. This ensures that the new sources also have a chance at being detected.

4) *Source Estimation*: Given the set of particles and associated weights, at any given point in time, we can compute estimates of source parameters by running a suitable clustering and evaluation technique. For autonomous operations, we usually run the source estimation stage after every s time steps of running the inner loop, unlike the traditional particle filter or the one proposed in [6], which run the prediction phase at each sensor reading. This not only saves on computation time, but also ensures that the estimates are made only after a significant portion of the map has been explored with high confidence.

We generate source parameter estimates from the particles by clustering them, and then representing the whole set by their respective cluster centroids. The clustering of the particles in \mathbb{A} can be done by any of the following methods:

- **Mean-shift Clustering**: This is a non-parametric feature-space algorithm widely used to locate the peaks of a density function [8]. It proceeds by fitting multi-variate Gaussians over the feature space and labeling the lobes as clusters. This step allows for multiple clusters, and hence enables the algorithm to localize multiple radiation sources. In addition, since the mean-shift technique groups based on the kernel parameters, and not the number of clusters, no information on the number of sources is required. A particular reason why this method works quite accurately is its robustness to Gaussian noise; since the kernel is a multi-variate Gaussian in itself, the clustering is robust to Gaussian noise - both due to the surroundings, and the one added by the algorithm during resampling.
- **Hierarchical Clustering**: Agglomerative HCA can be used for the classification of in the Euclidean space. HCA begins by placing each particle in a cluster of its own, and groups them into larger clusters, based on proximity in \mathbb{A} . This can be particularly useful for large particle populations, when mean-shift becomes computationally unfeasible. Various algorithmic manipulations enable agglomerative HCA to run in a worst case of $\mathcal{O}(n^2)$ [9], which makes up for the sub-optimal clustering.
- **ID-based Clustering**: Another naive way of

grouping particles can be based on the particle ID, a unique number given to every particle that was spawned in III-C1. When resampling occurs, some particles are respawned as other particles, and hence undergo a change in ID. Grouping based on this ID can serve as an inexpensive way to identify different clusters. This works amazingly well for very large environments, with a sparse distribution of sources - a case where the large particle population would make both the above algorithms computationally expensive. For denser environments, this technique fares poorly.

We propose the notion of *candidate sources*, which is the term used to refer to each of the cluster centroids identified by the clustering technique. These candidate sources are then screened, to eliminate spurious estimates and help improve the accuracy of classification. This also gives us the liberty to maintain a generic clustering algorithm that results in a large number of hypotheses, which can then be evaluated & classified, unlike [6], wherein the clustering algorithm would have to be fine-tuned to extract only the relevant sources.

5) *Source Labeling*: The last step of our algorithm evaluates the quality of candidate sources suggested by the clustering stage and decides whether the candidate can be labelled as a source, or dropped. We define the k^{th} -order confidence metric c_k for a candidate source p_c as follows.

$$c_k = \sum_{i=1}^k \omega_i p^* \left(m(S_i) | \mathcal{I}(S_i, p_c) \right) \quad (13)$$

where S_i , $1 \leq i \leq k$ are the k sensors nearest to the candidate source, $p^*()$ is same as defined in Eqn. (10), $\mathcal{I}()$ is as defined in Eqn. (1) and $\sum_i \omega_i = 1$. The weights, and k , are manually chosen, and can be optimised for best results.

This confidence measure is employed to test the credibility of the candidate source and make a decision on its acceptability - a candidate is declared as a resolved source *iff* its confidence score exceeds a predefined threshold. The knowledge of these resolved sources is then incorporated into the core algorithm as per Eqn. 11, to reinforce the computation and enable more accurate localization of the unresolved sources.

The Complete Picture: Bringing it all together, we have an algorithm that can localize multiple radiation sources sequentially, on two different levels. After the source estimation has been performed, candidate sources are evaluated based on the confidence metric c_k and labeled accordingly. In order to close the loop, and provide an end point to the algorithm, when necessary, we follow the

simple routine given by Alg. 1.

Algorithm 1: Closing the Loop

```

1 Function label_sources()
2   for  $p_c$  in candidate_sources do
3     if  $p_c^s \geq \text{source\_thresh}$  then
4       obtain confidence measure  $c_k$  from
         Eqn. (13);
5       if  $c_k \geq \text{confidence\_thresh}$  then
6         resolved_sources  $\leftarrow p_c$ ;
7   if checksum  $\geq \text{bg\_thresh}$  then
8     rerun the entire algorithm;
9   else
10    Exit algorithm (end point)

```

In the above algorithm, *bg_thresh* refers to the background radiation count of the environment and *checksum* is used as defined in section III-C2. The labelled sources are now classified as known sources and the algorithm uses them to localize sources further, as suggested in Eqn. (11).

IV. RESULTS

In this section, we present some of the results obtained by extending the algorithm described earlier to more complex cases. The core of the algorithm remains the same, as we extend the parameter space etc. We begin by demonstrating a sample run of the algorithm, as listed in the previous section, on simple cases.

Figure 6 illustrates one of the simplest possible scenarios, for multiple sources. Consider a $10m \times 10m$ environment, with 3 point sources with random parameters. Measurements are taken from a ground robot exploring the room in a lawnmower pattern. We proceed with random initialization, and exit the inner loop after 3 time steps. The estimation stage identifies 7 candidate sources (narrowband kernel chosen), which are then evaluated to resolve all the sources in a single iteration. (*Confidence Score* $c_3 = \{96\%, 90\%, 98\%\}$; *Run-time* = 33.2s)

Figure 7 illustrates the real reason why the proposed algorithm fares well in localizing multiple sources. The setup is similar to the previous example, with 3 sources randomly positioned in the same grid. After 3 time steps, the algorithm identifies 8 clusters, and on evaluating them using c_3 , the algorithm only manages to localize 2 out of these. The third source could not be captured by the particles with a good confidence score. Hence, the two sources are marked as resolved, and the inner

loop is called again. After a second round of filtering, the algorithm manages to localize the third source with much higher confidence of 93.7%, establishing our idea. After a portion of the sources have been localized, the localization task is, in fact, simpler, and thus the efficiency of the algorithm improves. State-of-the-art implementations would have either failed to capture the third source, or done so with a much higher localization error.

(Confidence Scores $c_3 = \{87\%, 85\%, 94\%\}$; Runtime = 64.0s)

A. Localizing Bulk Sources

Most of the existing algorithms fail to address the task of localization of bulk sources, or similar source distributions. Some existing approaches propose an extension, by approximating a bulk source by its equivalent point source representation. This approximation only holds for very large distances and gives inaccurate and unreliable parameter estimates for short distances, especially in closed environments. Taking inspiration from electromagnetism, we can claim that particle flux, like any other $1/R^2$ field following the principle of superposition, due to a source distribution can be broken down into its corresponding monopole, dipole, quadrupole moments and so on [15]. The electric potential at a point P due to a charge distribution with total charge Q_0 , dipole moment \mathbf{P} and quadrupole moment Q_q , at a distance r from P can be given as:

$$V_0(P) = \frac{1}{4\pi\epsilon_0} \frac{Q_0}{r} + \frac{1}{4\pi\epsilon_0} \frac{\mathbf{P} \cdot \hat{\mathbf{r}}}{r^2} + \frac{1}{4\pi\epsilon_0} \frac{Q_q}{r^3} \quad (14)$$

The electric field can be computed as the derivative of this potential as $-\frac{\partial V_0}{\partial r}$. This expression clearly shows why the point source assumptions fail at small values of r .

Since the proposed algorithm just involves estimation of the parameter vector \mathbf{A}_k , we can increment the dimension of \mathbf{A}_k , at the cost of runtime/compute power, to achieve similar results. A setup with a wall-type bulk source was simulated in the same environment as before, to validate the idea. By incorporating the dipole contributions alone, the algorithm was able to localize the distribution with a whopping c_5 of 99.2%, in 4 time steps and a runtime of 81s. The increase in runtime is because of the added dimension, which causes the mean-shift clustering algorithm to blow up.

B. Scaling to 3-D

A very important aspect for any localization algorithm is its scalability. In our case, to maintain

the same density of coverage in parameter space \mathbb{A} , the number of particles required blows up exponentially with dimensions. This in turn, would blow up the clustering time and overall runtime beyond bounds. To account for these, we propose guided initialization of the particles, as suggested in III-C1. Information from other sensors on the robot, like visual imagery, laser scans etc. can be used to form saliency maps, which can be used to cleverly initialize particles in \mathbb{A} . As an example, we consider the case of a closed room, whose point cloud was borrowed from [21]. Sources were placed at locations corresponding to the sofa and a wooden cabinet, and particles were initialized by undersampling the point cloud of the scene. The algorithm successfully localizes the two sources (Fig. 9) in 3 time steps, and a runtime of 39s, hence ascertaining the scalability to higher dimensional regions.

C. Field Test

The algorithm was experimentally verified using the particle flux measurements obtained from the CdZnTe-based Polaris-H camera [7], mounted on top of the *Lilred* ground robot, complete with a Velodyne LIDAR, visual camera, wheel odometry and thermal camera amongst other things. The results of the algorithm can be seen in figure 10(d), where it localizes the single point source ($100\mu Ci$, Cs-137) in 3 time steps (runtime = 37s).

D. Quantitative Analysis

We consider a simulated 2-D environment, with 500 particles and a single point source. The analysis of confidence score c_3 and localization error ϵ_l is given by 11(a). Here, ϵ_l is defined as:

$$\epsilon_l = (\Delta A^{pos})^2 + (\Delta A^{str})^2 \quad (15)$$

where A^{pos} is the position in cm, A^{str} is the source intensity in μCi , and Δ refers to the difference between ground truth and estimated source parameters. Clearly, the drop in localization error is stagnant after 3/4 time steps, and hence we break every iteration at 3/4 time steps before entering the source estimation stage.

Figure 11(b) shows the 2-D v/s 3-D analysis of the algorithm. With suitable initialization, it is shown that the algorithm can scale seamlessly to higher dimensions, unlike the exponential trend expected otherwise.

Table I shows a comparative analysis of the proposed algorithm, against the improved particle filter-based implementation suggested by [6]. The environment used is a 2-D square grid of edge length 20m, with 100 measurements and 1000

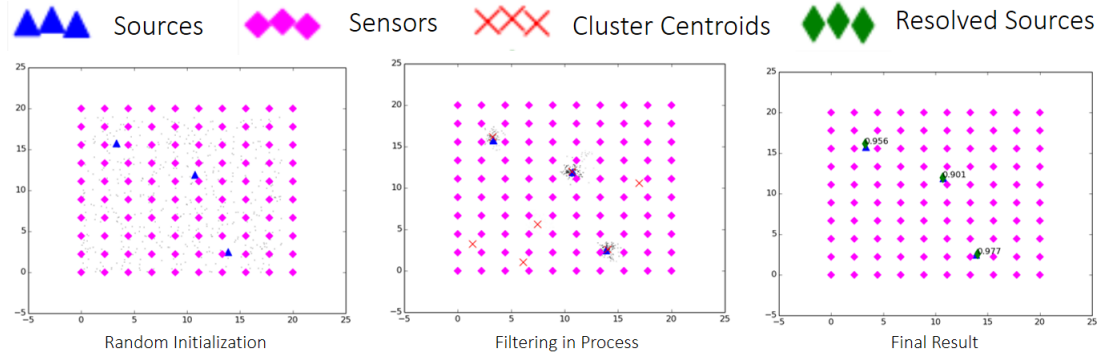


Fig. 6: Sample run of the algorithm in 2-D space, with 3 sources and 100 readings. *Algorithm terminates in 3 time steps (1 iteration).*

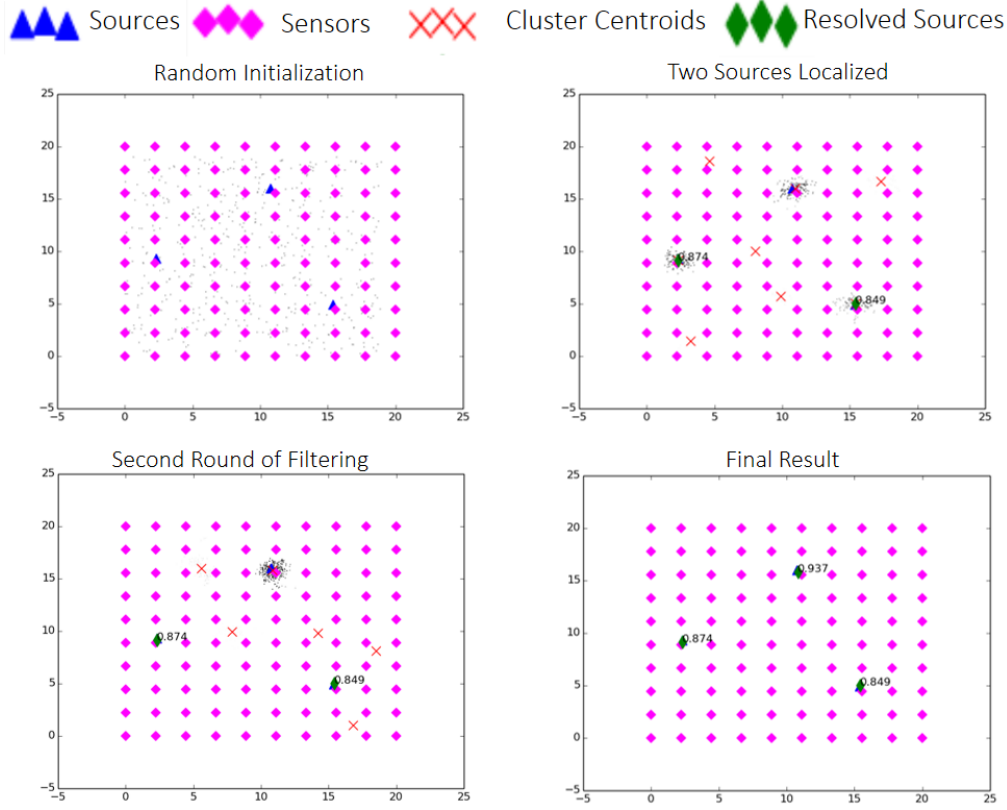


Fig. 7: Sample run of the algorithm in 2-D space, with 3 sources and 100 readings. *Algorithm terminates in 6 time steps (2 iterations).*

Configuration	Existing						Proposed					
	Time Steps	Iterations	Localization Error	Precision	Recall	F1	Time Steps	Iterations	Localization Error	Precision	Recall	F1
1 Source	4	1	0.146	0.96	1	0.980	2	1	0.163	0.99	0.99	0.990
							3	1	0.147	0.99	1	0.995
2 Sources	4	1	0.321	0.9626	0.935	0.949	3	1.11	0.289	0.975	0.975	0.975
							4	1.07	0.277	0.995	0.975	0.985
3 Sources	4	1	1.259	0.759	0.7503	0.755	4	1.67	0.742	0.964	0.9663	0.965
	5	1	1.118	0.7695	0.8004	0.785	5	1.63	0.748	0.9766	0.973	0.975
4 Sources	5	1	-	0.607	0.495	0.545	4	2.75	1.214	0.9629	0.9408	0.952

TABLE I: Comparative study of proposed algorithm with state-of-the-art.

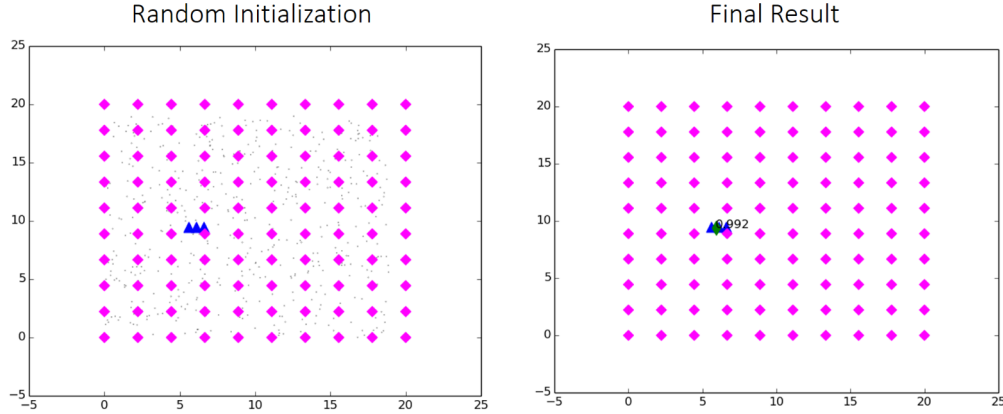


Fig. 8: Sample run of the algorithm in 2-D space, localizing a wall-type bulk source. *Algorithm terminates in 3 time steps (1 iteration).*

particles. The values mentioned were averaged over 100 executions of the algorithm, for each source configuration.

We see that the algorithm barely shows any improvement over the existing method, when the iteration count is 1 - this is clearly because the inner loop of the algorithm is conceptually the same. Due to subtleties of implementation, we do have faster convergence, but the real contributions of the algorithm are only visible when the number of iterations go beyond one. Especially for a 3/4 source localization case, as reported, we see a tremendous improvement over the existing algorithm, as the number of iterations approach 2 and more. The improvements in localization error and F1 scores clearly shows the contributions of the outer loop of the algorithm.

As for the running time, the existing approach reports about 0.22s per sensor reading, on a 2.40 GHz Intel Core 2 Quad personal computer with 2 GB of RAM, amounting to 43.12s for a 196 sensor grid. Running a similar setup with 196 sensor measurements and 2000 particles on a 1.80 GHz AMD A10 Quad processor with 8 GB of RAM, takes 32s for 3 time steps, involving just one clustering routine. Even after accounting for the improvement in RAM and lower clock frequency, the proposed algorithm runs faster than the existing algorithm.

E. Conclusion

We have addressed the problem of robust localization of multiple radiation sources, and distributions thereof, using a mobile robot with consideration of noise and uncertainties. Unlike existing algorithms, the proposed algorithm can also be extended to complex environments, for the local-

ization of bulk sources, for example, and is scalable to large environment sizes and higher dimensions. The proposed algorithm is robust to sensor failure, uncertainties in measurement or odometry, and is independent of the path chosen for exploration of the environment. The algorithm can localize very large number of sources, with high certainty, and the complexity & running times scale reasonably with the source distribution. Results from simulation and field tests verified the accuracy of our algorithm in a number of realistic scenarios, and show significant improvement over the state-of-the-art.

V. FUTURE WORK

The aim of our work is to generate a multi-modal map of an enclosed environment, which includes radiation mapping along with thermal maps, laser scans etc. The radiation mapping would require localization and estimation of large volumes of radioactive materials, distributed in a large environment.

With this work, we have showed a method for localization of multiple point & bulk sources, especially a large number of them, in a closed environment and demonstrated scalability. Further work would involve tests in 3-D environments with aerial robots, coupled with other sensors for guided initialization, for testing efficiency in 3-D.

Another viable extension would be to modify the algorithm into an active localization algorithm, which can explore the environment autonomously, using feedback from the radiation sensor measurements. Seeking inspiration from acoustic localization, DoA-based algorithms may also be extended for this setup. A particular application would be to

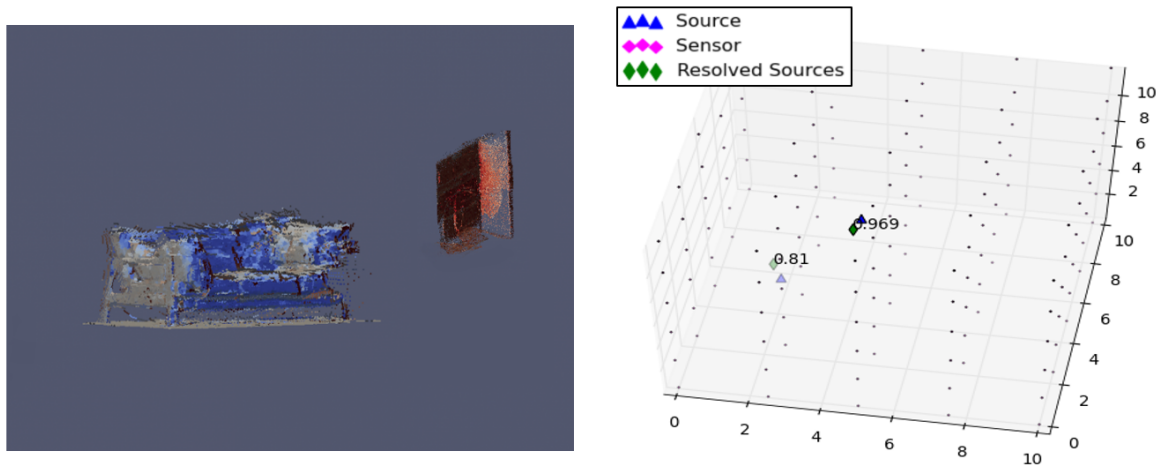


Fig. 9: Sample run of the algorithm in 3-D space, with guided initialization using point cloud (left). Algorithm terminates in 3 time steps (1 iteration).

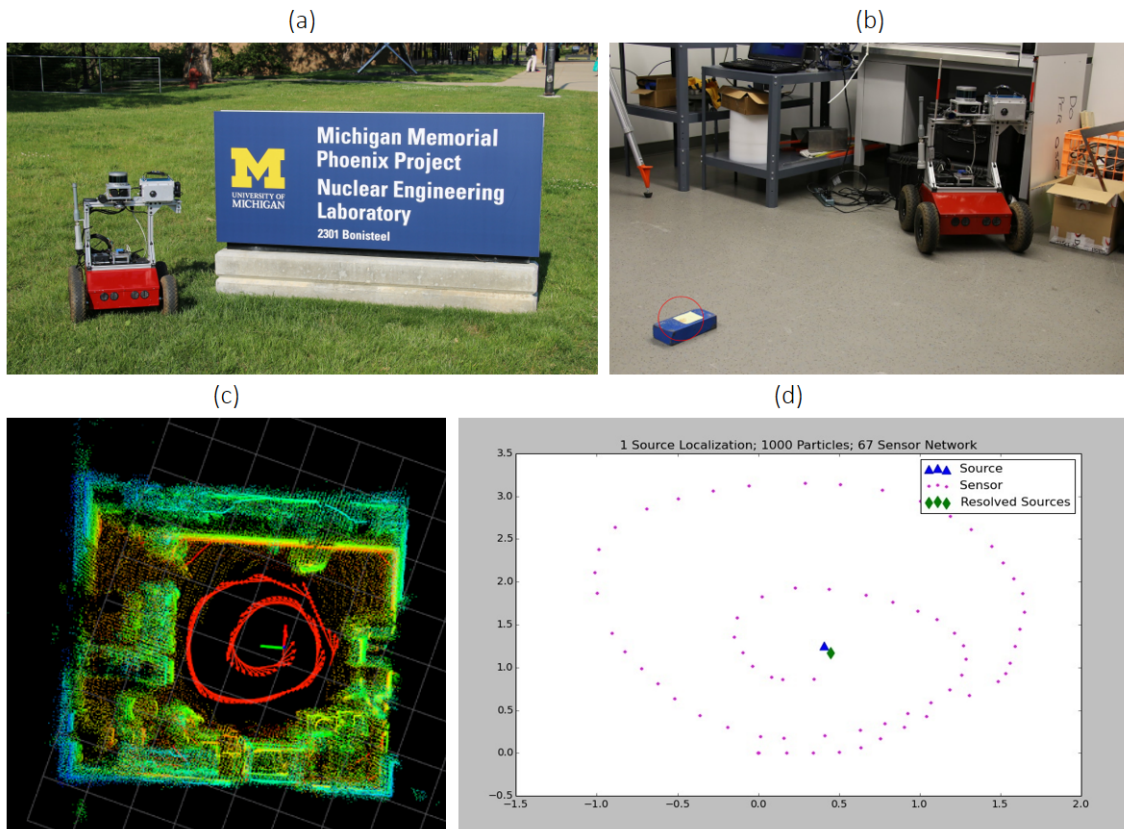


Fig. 10: Field test at Phoenix Memorial Laboratories: (a) ground robot used; (b) picture from the test (source encircled in red); (c) point cloud of the room (path in red); (d) results of the localization algorithm.

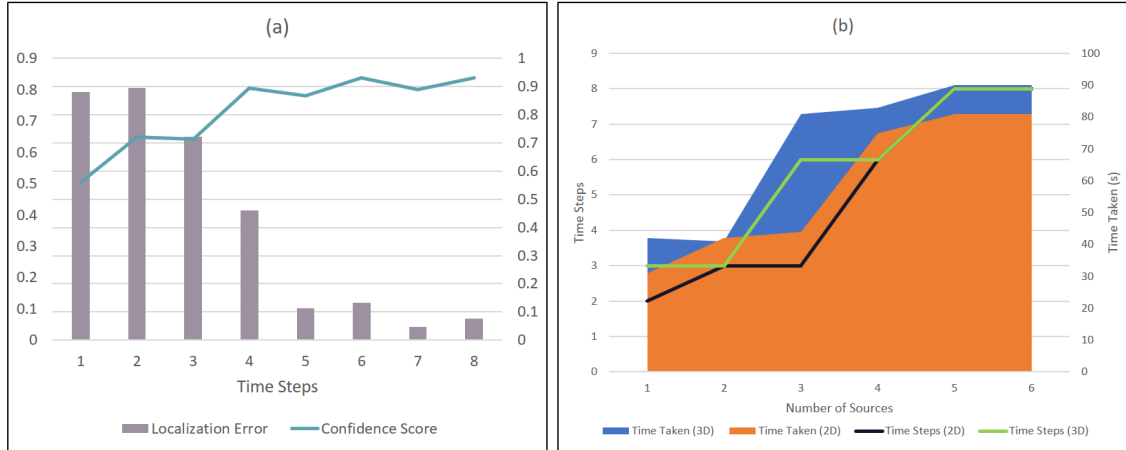


Fig. 11: (a) Analysis w.r.t. time steps, and (b) 2-D v/s 3-D analysis.

use the particle flux measurements for homing in on the sources, using aerial robots.

REFERENCES

- [1] M. S. Arulampalam, S. Maskell, N. Gordon, and T. Clapp. A tutorial on particle filters for online nonlinear/non-gaussian bayesian tracking. *IEEE Transactions on Signal Processing*, 50(2):174–188, Feb 2002.
- [2] H. E. Baidoo-Williams. Maximum Likelihood Localization of Radiation Sources with unknown Source Intensity. *ArXiv e-prints*, July 2016.
- [3] H. E. Baidoo-Williams, S. Dasgupta, R. Mudumbai, and E. Bai. On the gradient descent localization of radioactive sources. *IEEE Signal Processing Letters*, 20(11):1046–1049, Nov 2013.
- [4] Eric Thomas Brewer. Autonomous localization of $1/r^2$ sources using an aerial platform. Master’s thesis, Virginia Polytechnic Institute and State University, Blacksburg, Virginia, 2009.
- [5] Yang Cheng and Tarunraj Singh. Source term estimation using convex optimization. In *2008 11th International Conference on Information Fusion*, pages 1–8, June 2008.
- [6] J. C. Chin, D. K. Y. Yau, and N. S. V. Rao. Efficient and robust localization of multiple radiation sources in complex environments. In *2011 31st International Conference on Distributed Computing Systems*, pages 780–789, June 2011.
- [7] Jiyang Chu, Michael Streicher, Jeffrey A. Fessler, and Zhong He. Unbiased filtered back-projection in 4 compton imaging with 3d position sensitive detectors. PP:1–1, 09 2016.
- [8] D. Comaniciu and P. Meer. Mean shift: a robust approach toward feature space analysis. *IEEE Transactions on Pattern Analysis and Machine Intelligence*, 24(5):603–619, May 2002.
- [9] William H. E. Day and Herbert Edelsbrunner. Efficient algorithms for agglomerative hierarchical clustering methods. *Journal of Classification*, 1(1):7–24, Dec 1984.
- [10] Min Ding and Xiuzhen Cheng. Fault tolerant target tracking in sensor networks. In *Proceedings of the Tenth ACM International Symposium on Mobile Ad Hoc Networking and Computing*, MobiHoc ’09, pages 125–134, New York, NY, USA, 2009. ACM.
- [11] Nathaniel Fairfield. *Localization, Mapping, and Planning in 3D Environments*. PhD thesis, Robotics Institute, Carnegie Mellon University, Pittsburgh, PA, January 2009.
- [12] A. Gunatilaka, B. Ristic, and R. Gailis. On localisation of a radiological point source. In *2007 Information, Decision and Control*, pages 236–241, Feb 2007.
- [13] Samuel W. Hasinoff. *Photon, Poisson Noise*, pages 608–610. Springer US, Boston, MA, 2014.
- [14] J. W. Howse, L. O. Ticknor, and K. R. Muske. *Least squares estimation techniques for position tracking of radioactive sources*. November 2001.
- [15] Mark Jarrell. Graduate electrodynamics.
- [16] Robert E. Kass and Adrian E. Raftery. Bayes factors. *Journal of the American Statistical Association*, 90(430):773–795, 1995.
- [17] M. Morelande, B. Ristic, and A. Gunatilaka. Detection and parameter estimation of multiple radioactive sources. In *2007 10th International Conference on Information Fusion*, pages 1–7, July 2007.
- [18] M. R. Morelande, C. M. Kreucher, and K. Kastella. A bayesian approach to multiple target detection and tracking. *IEEE Transactions on Signal Processing*, 55(5):1589–1604, May 2007.
- [19] M. R. Morelande and B. Ristic. Radiological source detection and localisation using bayesian techniques. *IEEE Transactions on Signal Processing*, 57(11):4220–4231, Nov 2009.
- [20] Ruixin Niu and Pramod K. Varshney. Distributed detection and fusion in a large wireless sensor network of random size. *EURASIP J. Wirel. Commun. Netw.*, 2005(4):462–472, September 2005.
- [21] François Pomerleau, M. Liu, Francis Colas, and Roland Siegwart. Challenging data sets for point cloud registration algorithms. *The International Journal of Robotics Research*, 31(14):1705–1711, December 2012.
- [22] N. S. V. Rao, M. Shankar, J. C. Chin, D. K. Y. Yau, C. Y. T. Ma, Y. Yang, J. C. Hou, X. Xu, and Sartaj Sahni. Localization under random measurements with application to radiation sources. In *2008 11th International Conference on Information Fusion*, pages 1–8, June 2008.
- [23] Thrun Sebastian. Particle filters in robotics. In *Proceedings of the Eighteenth Conference on Uncertainty in Artificial Intelligence*, UAI’02, pages 511–518, San Francisco, CA, USA, 2002. Morgan Kaufmann Publishers Inc.
- [24] Wikipedia. Radiation, 2004. [Online; accessed 22-July-2004].
- [25] Yi Zou and Krishnendu Chakrabarty. Sensor deployment and target localization in distributed sensor networks. *ACM Trans. Embed. Comput. Syst.*, 3(1):61–91, February 2004.